# Decadal Variability & Impact of the Kuroshio Extension System

**Bo Qiu, Shuiming Chen & Niklas Schneider**

**Department of Oceanography, University of Hawaii, USA**

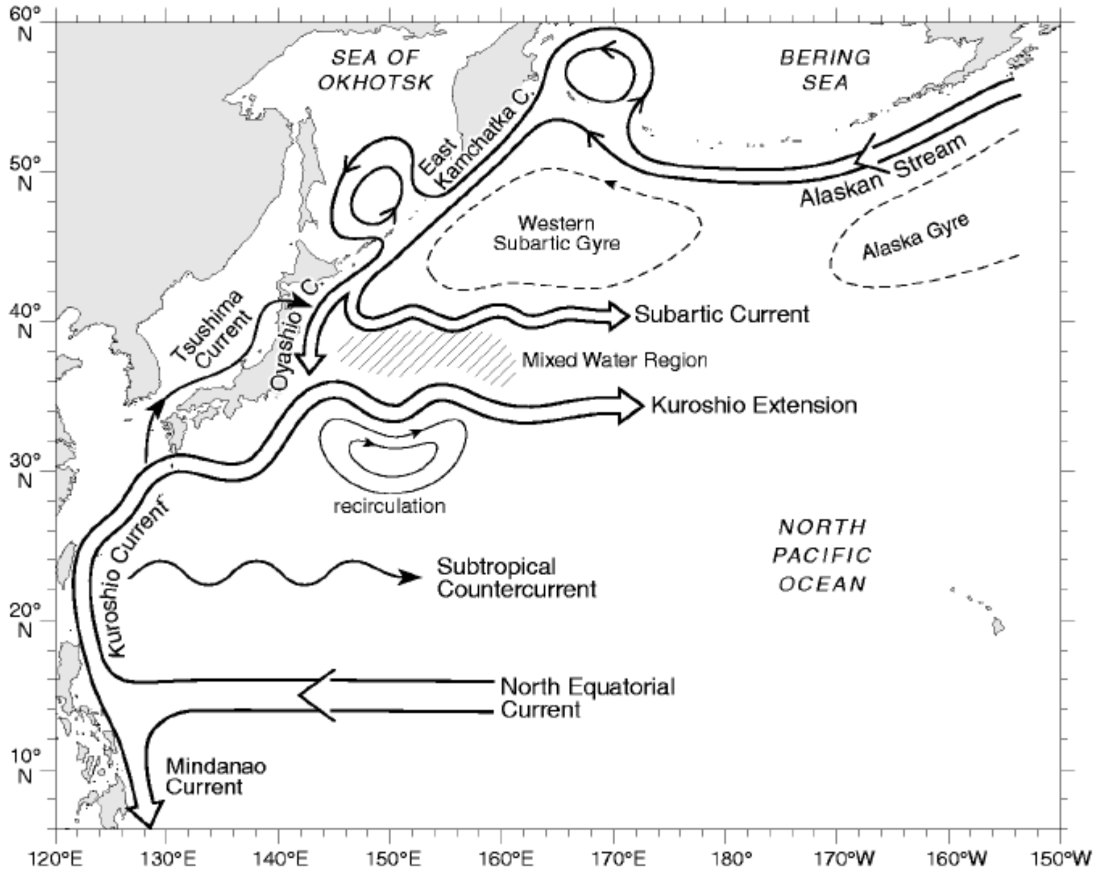


US CLIVAR

**Ocean Carbon Hot Spots Workshop, MBARI, 25-26 September 2017**

# KE has the highest mesoscale eddy variability in the Pacific Ocean

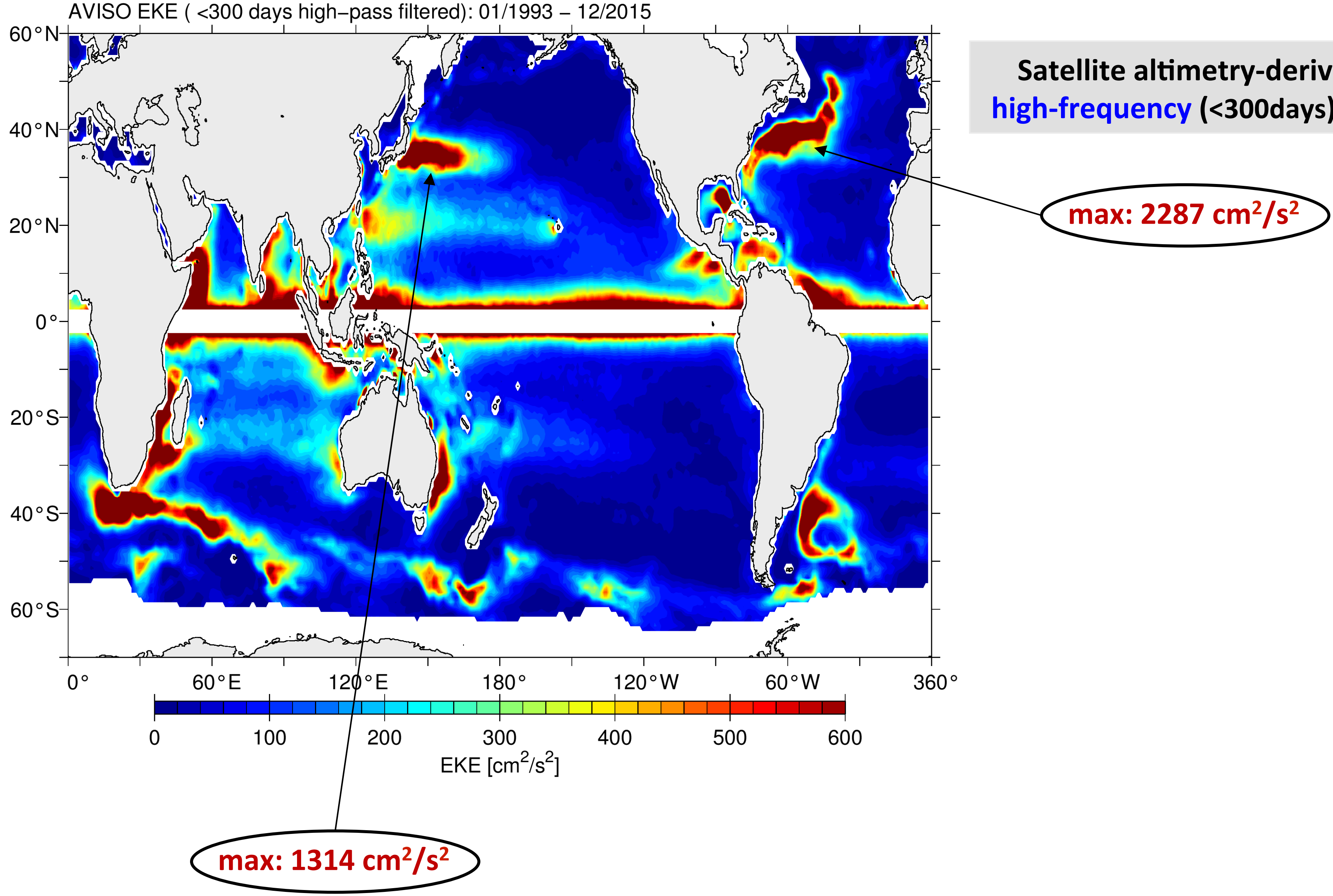


**Satellite altimetry-derived high-frequency (<300days) EKE**

# KE has the highest low-frequency circulation variability in world oceans

**Satellite altimetry-derived**
**high- vs. low-frequency EKE**

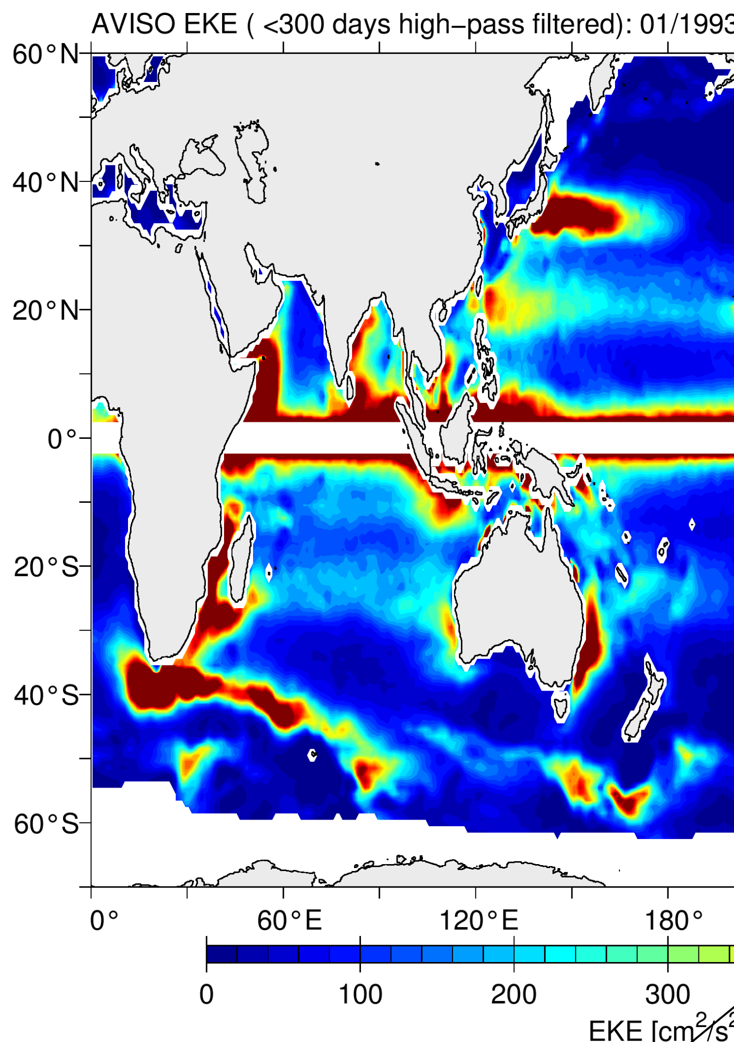


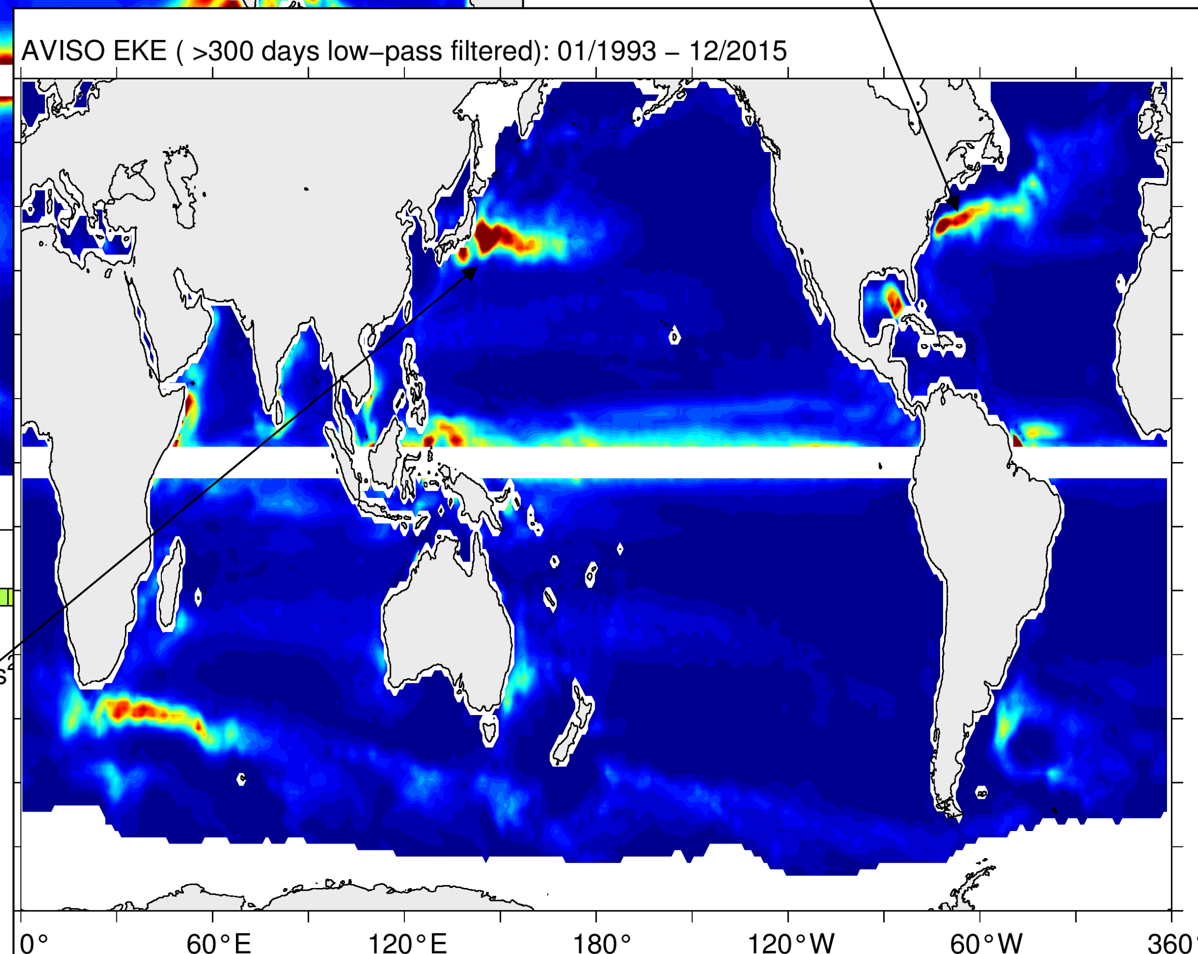

# Outlines

- Observed decadal variability — introducing KE index
- KE decadal variability as "externally" wind-forced response
- Impact on subtropical mode water & regional SST gradient
- Mechanism underlying the decadal KE variability

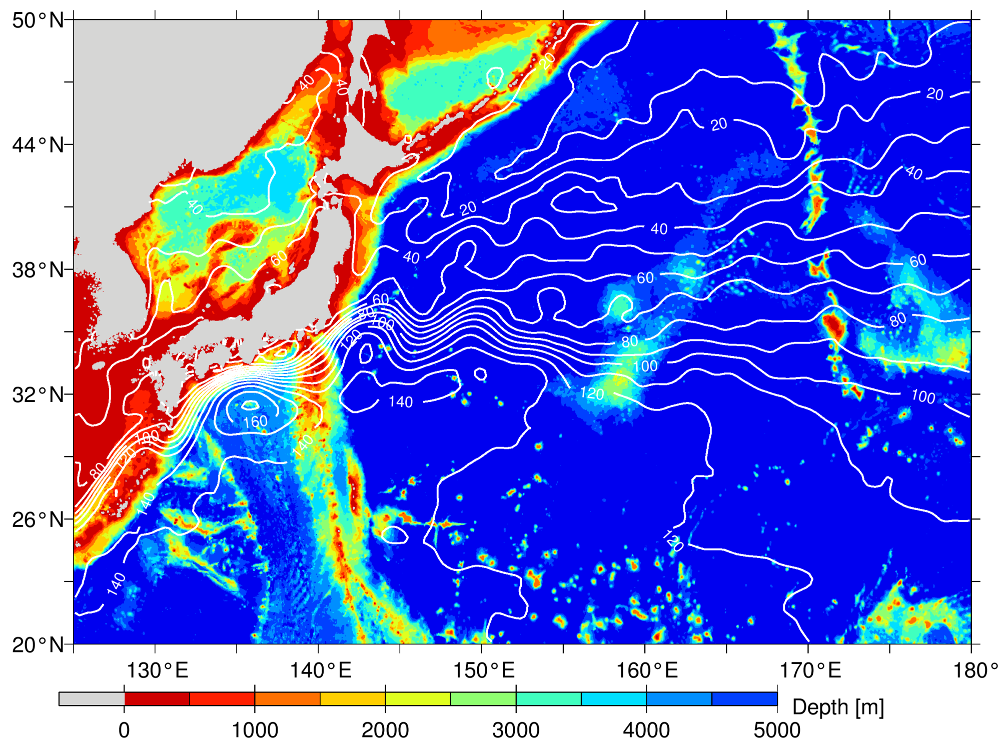


SSH field and topography in the KE region

# Yearly maps of bi-weekly paths of the Kuroshio/KE jet

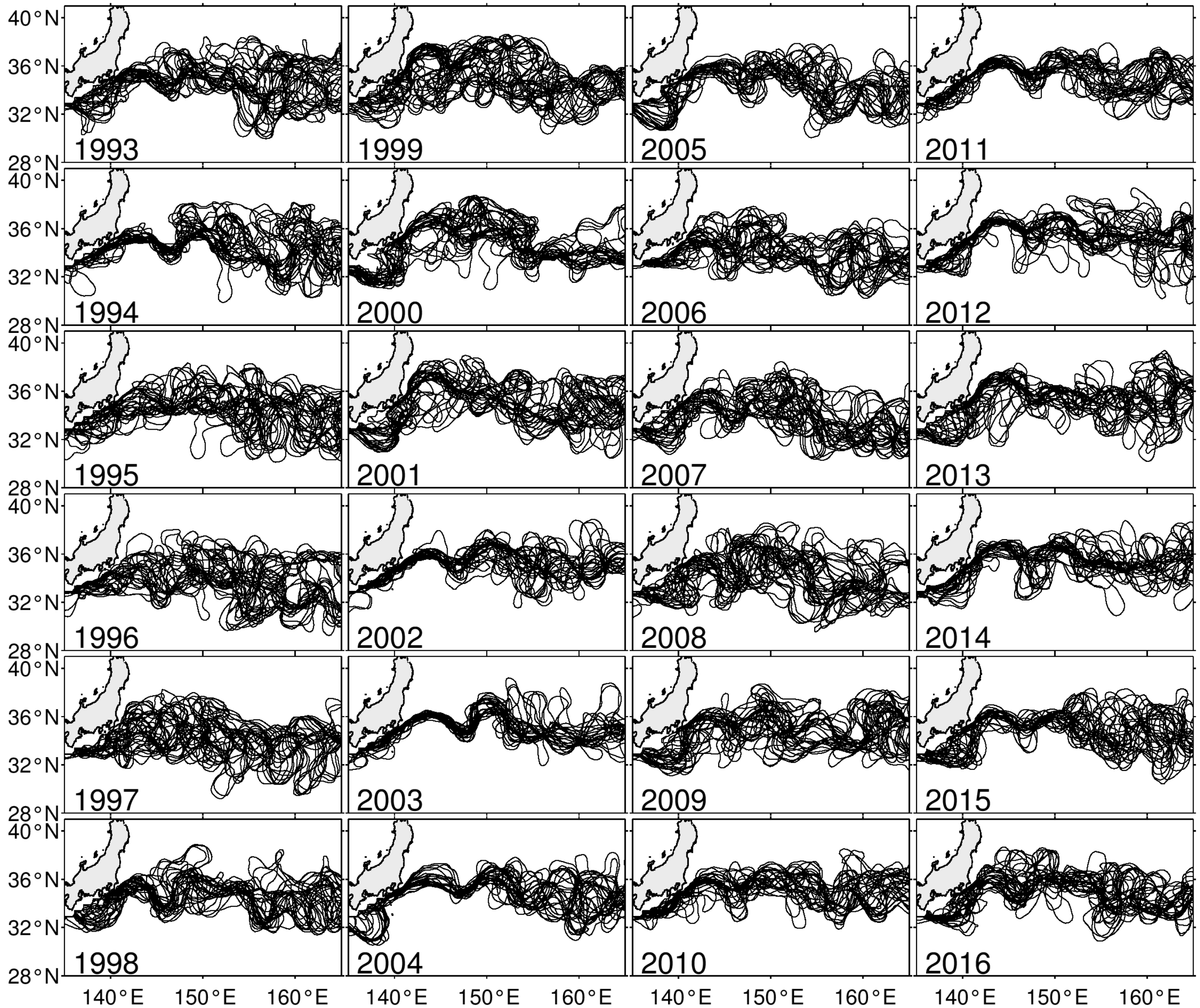


**Alternation between stable versus unstable states**

# Dynamically stable vs. unstable phases of the KE system

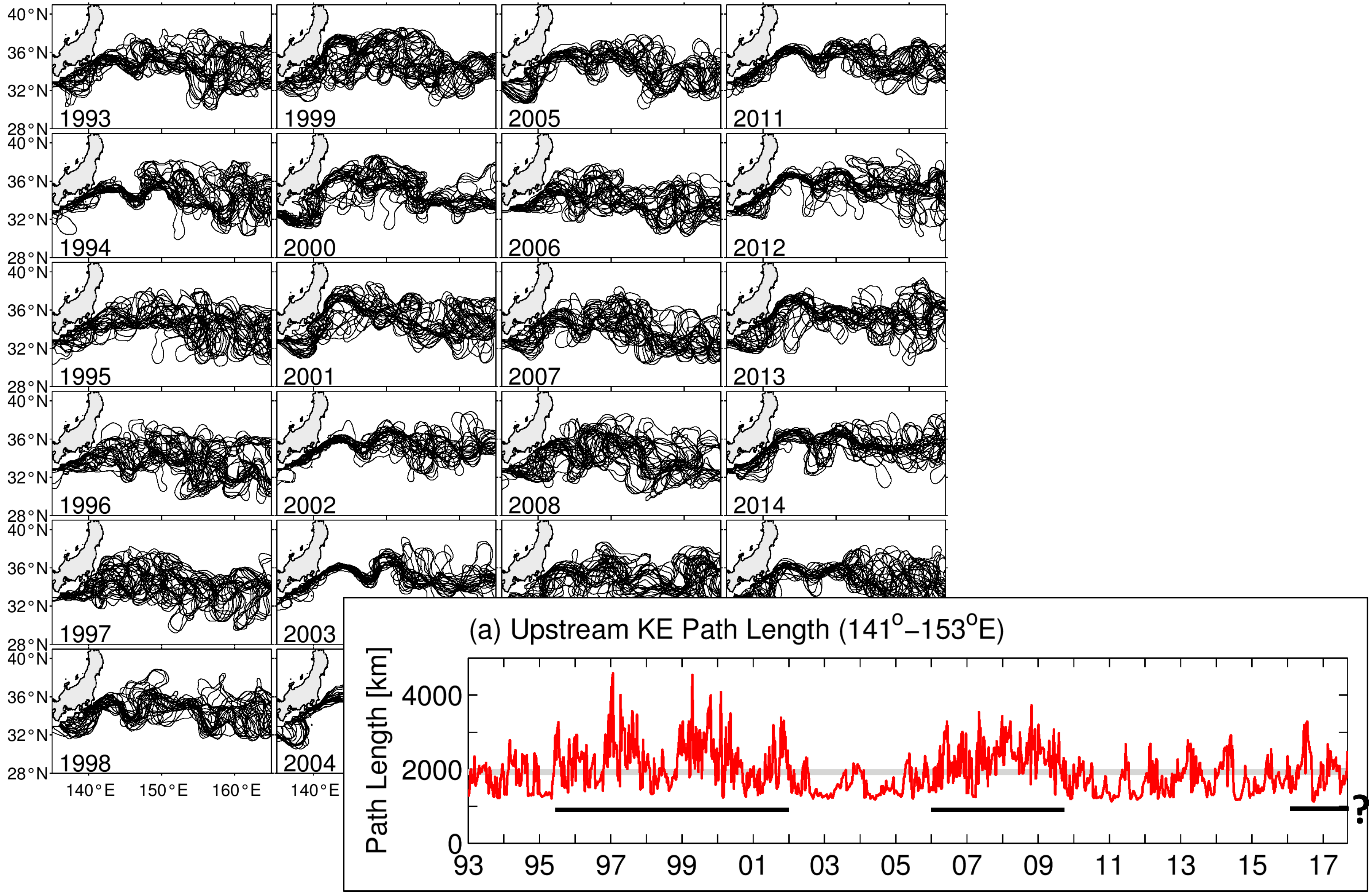


**Stable yrs: 1993-94, 2002-04, 2010-15**

**Unstable yrs: 1996-2001, 2006-09**

# Other dynamical quantities representing the decadal KE variability

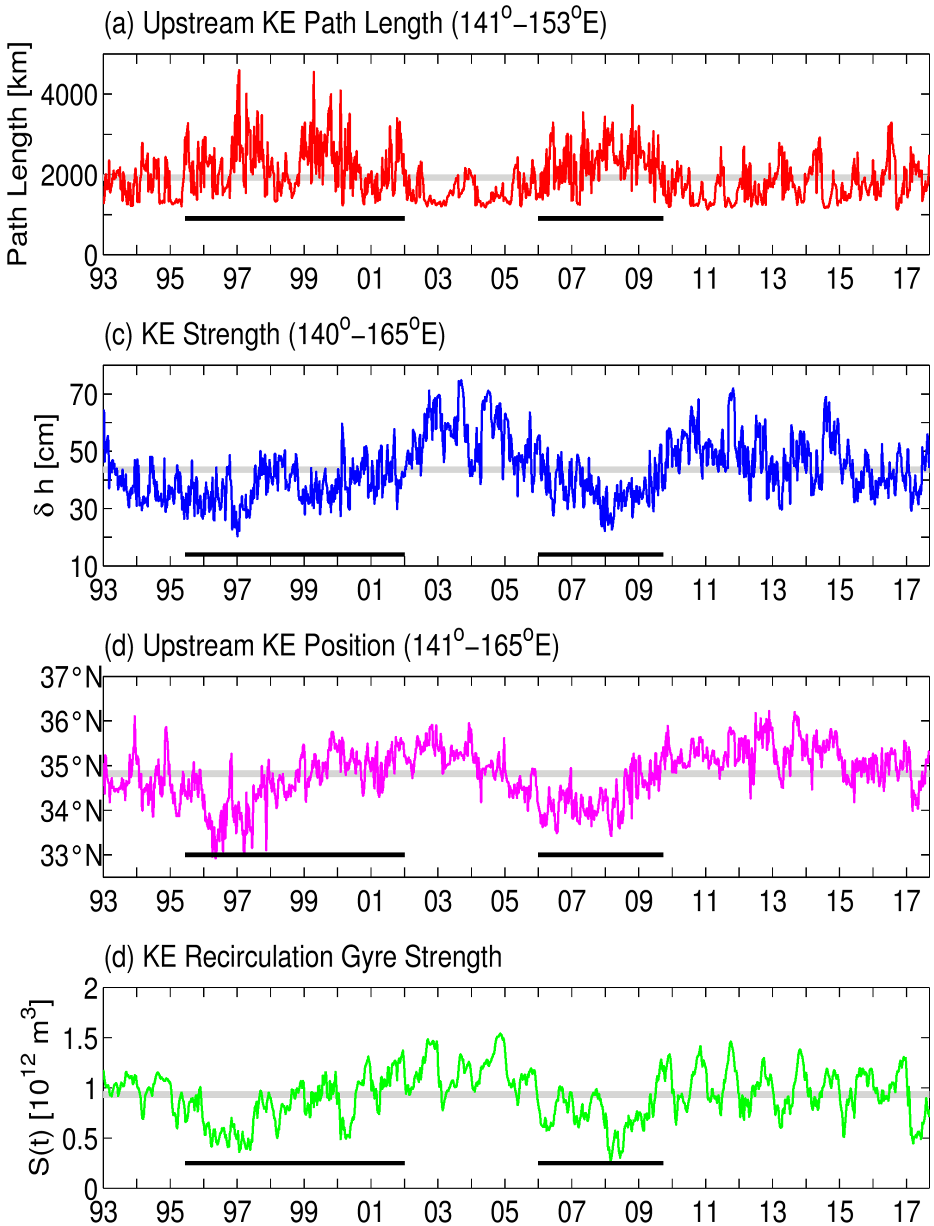


**Typical yearly SSH patterns in unstable/contracted vs. stable/elongated phases**

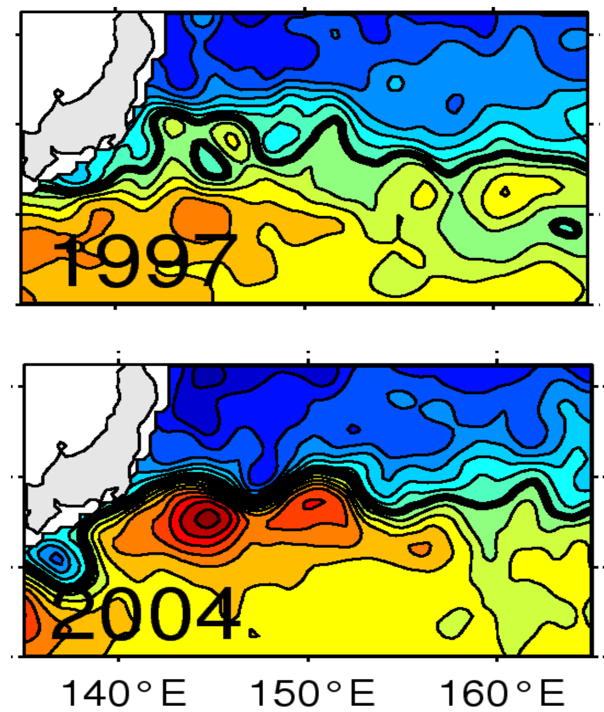

# Forming of a comprehensive index representing the KE variability

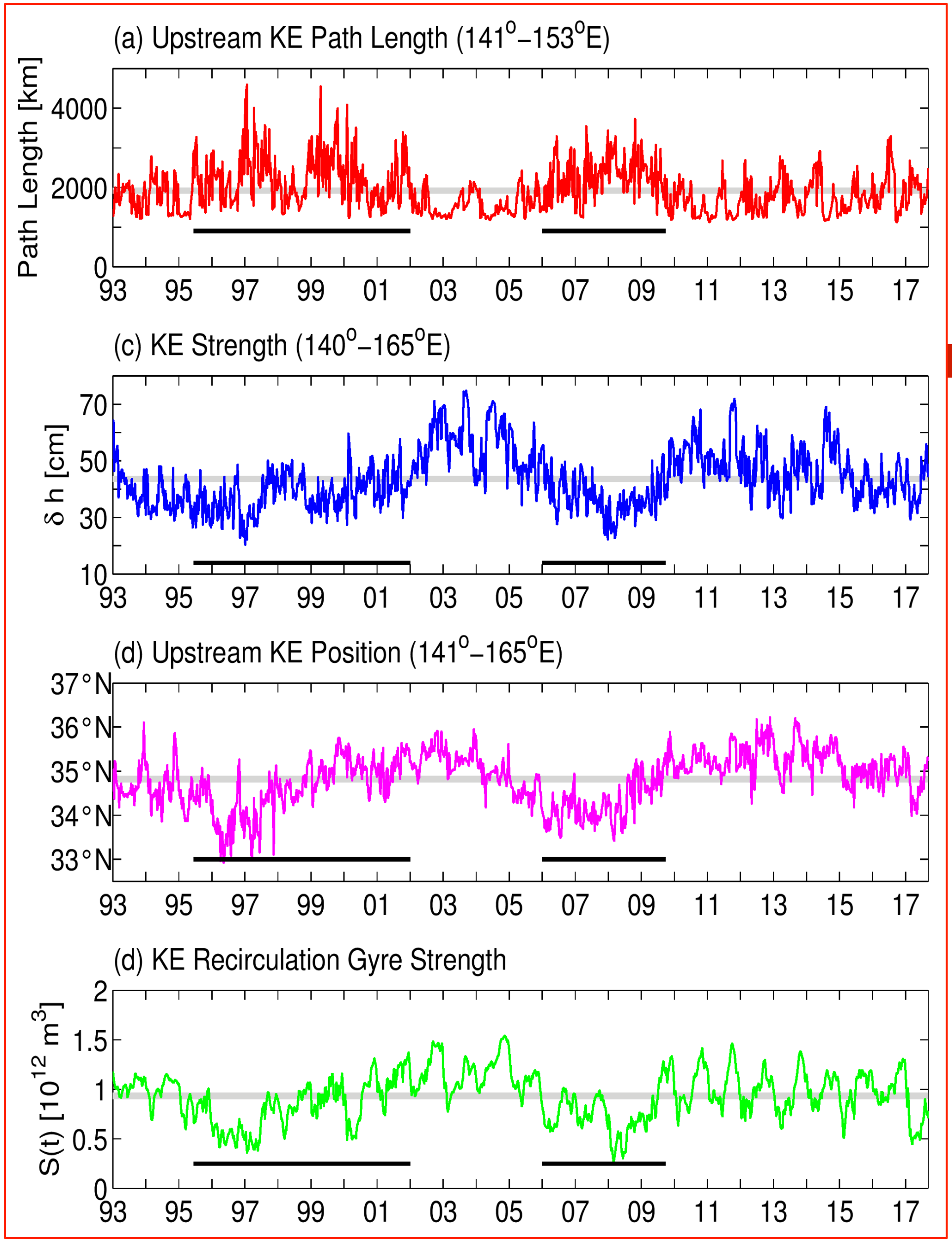


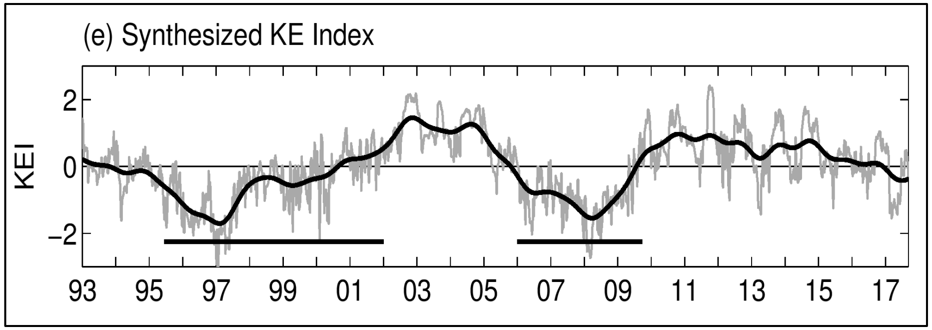


**KE index : average of the 4 dynamical quantities (normalized)**

**Qiu et al. (2014, JClim)**

# Regression between the KE index and basin-wide SSH anomaly field

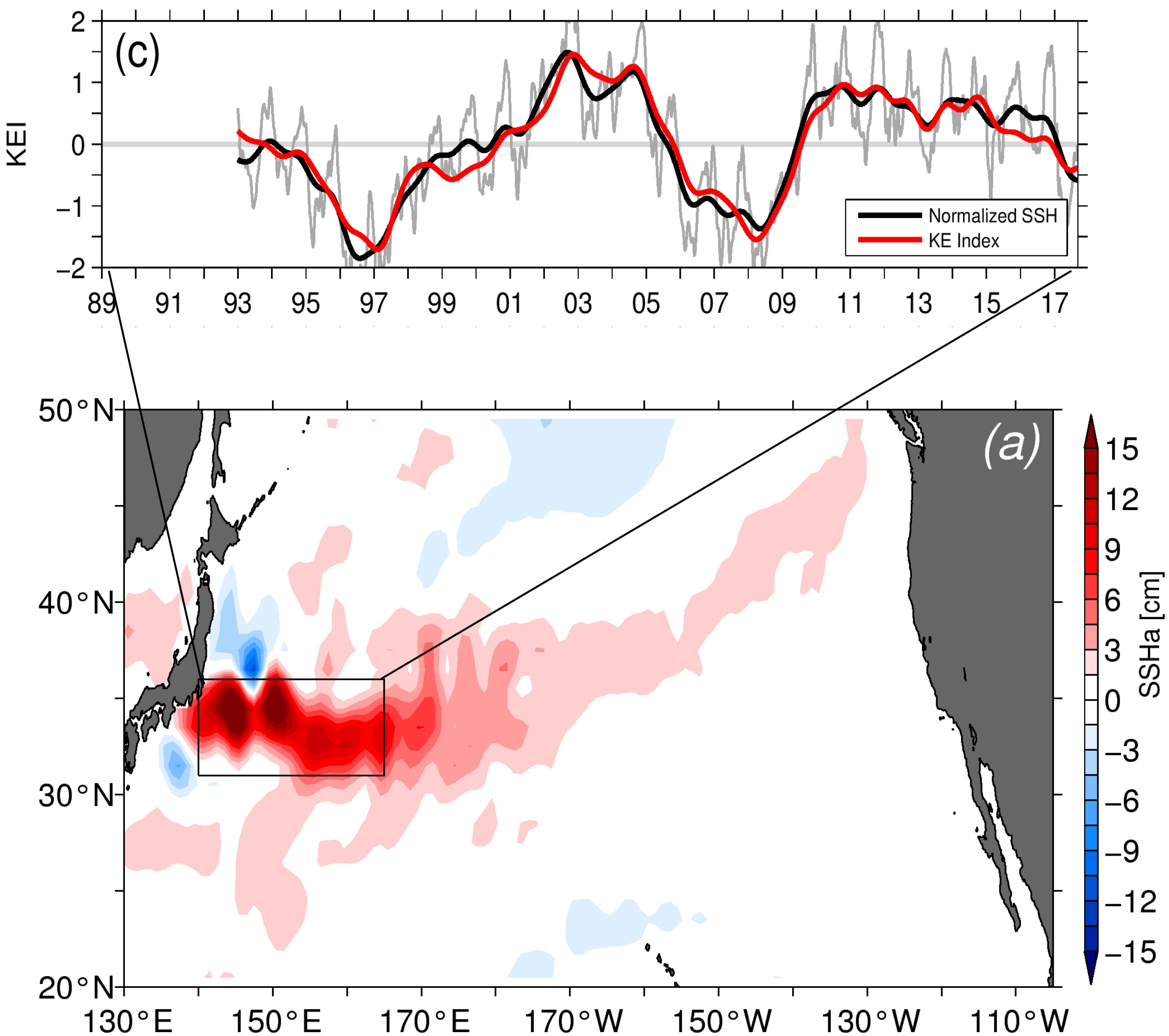


**KE index: represented well by SSH anomalies in the southern RG box (31-36°N, 140-165°E)**

**KE index from dynamical properties**

**box-averaged SSH time series**

# Regression between the KE index and basin-wide SSH anomaly field

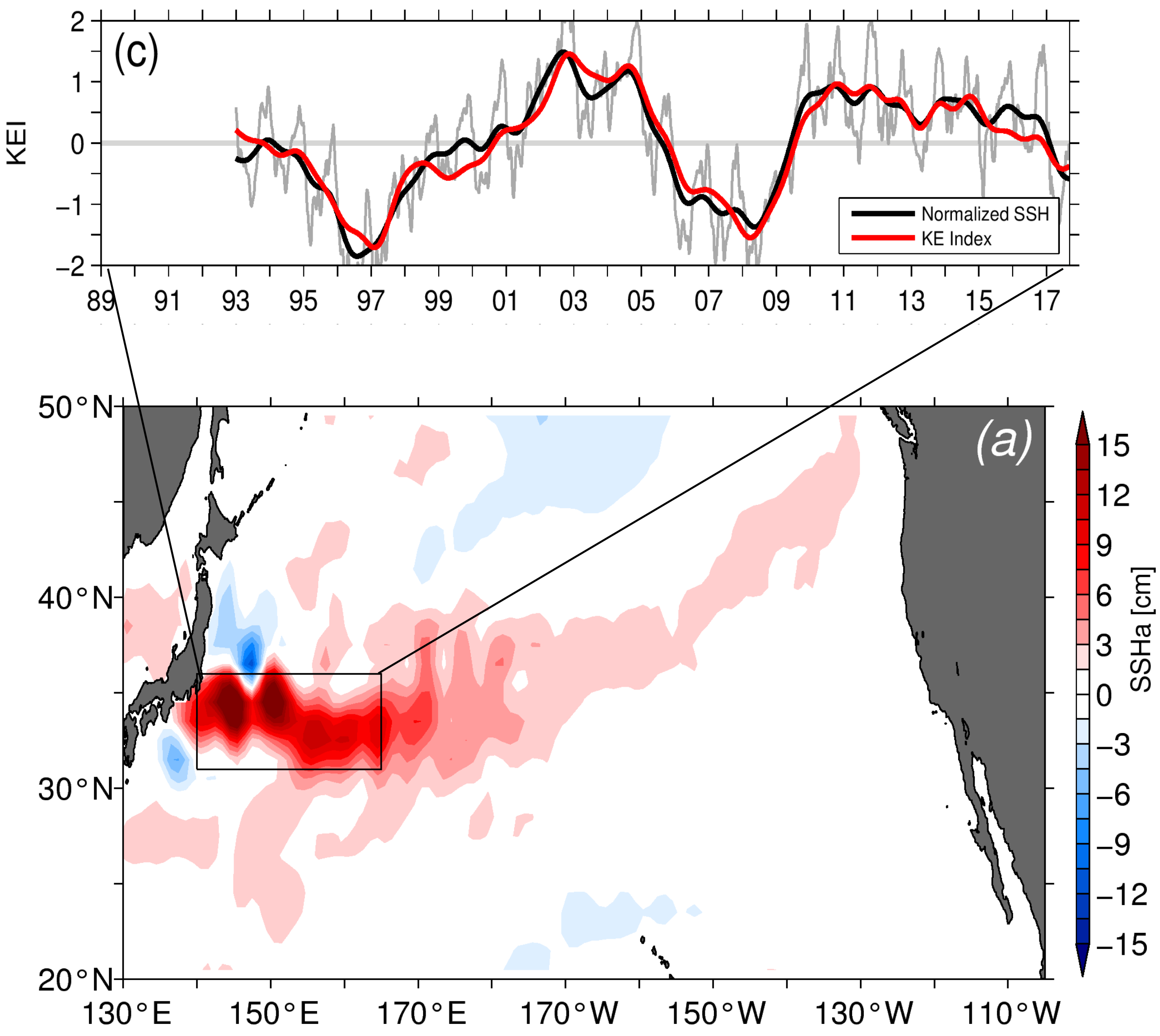


**KE index: represented well by SSH anomalies in the southern RG box (31-36°N, 140-165°E)**

## Implications

- **Examining KE index becomes equivalent to examining SSH anomalies in this key box**
- **Dynamically, it is easier to explore SSH changes than circulation/eddy variations**
- **Midlatitude SSH changes are largely governed by wind-forced baroclinic adjustment**

# Decadal KE variability lags the negative PDO index by ~ 3 years ( r = 0.74 )

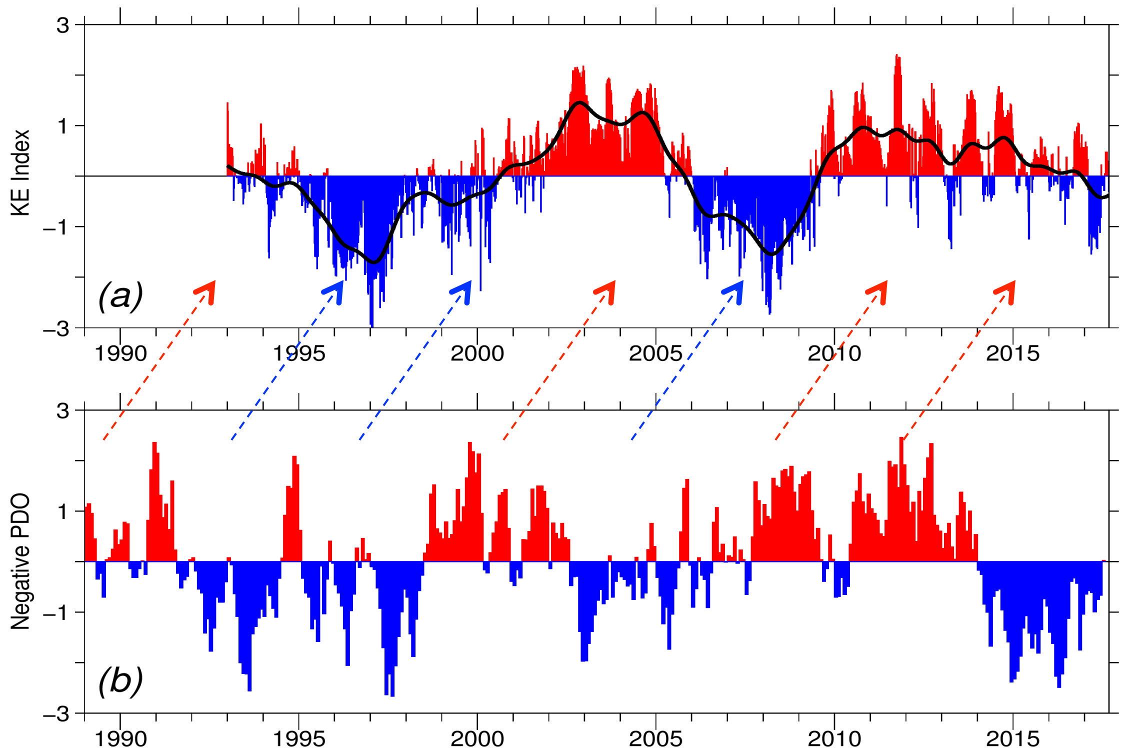


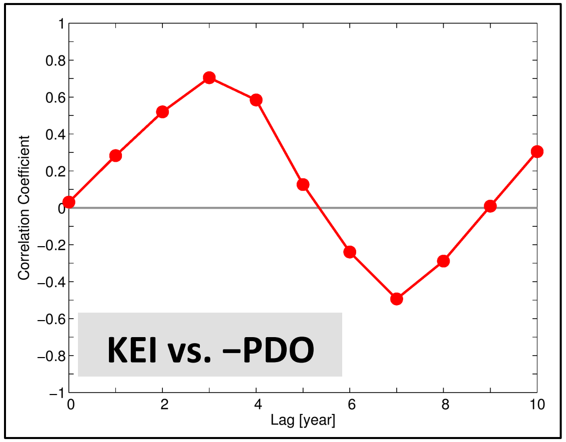


- Center of PDO wind forcing is in eastern half of the N Pacific basin
- - PDO corresponds to a weakened Aleutian Low that generates + SSHAs through Ekman convergence
- 3~4-yr lag is the cross-basin adjustment time

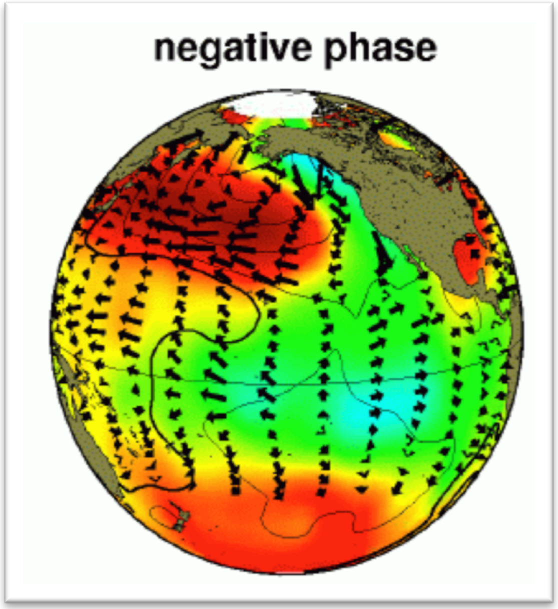


Mantua et al. (1997, BAMS)

# Connections between PDO forcing, cross-basin SSH adjustment & KE index

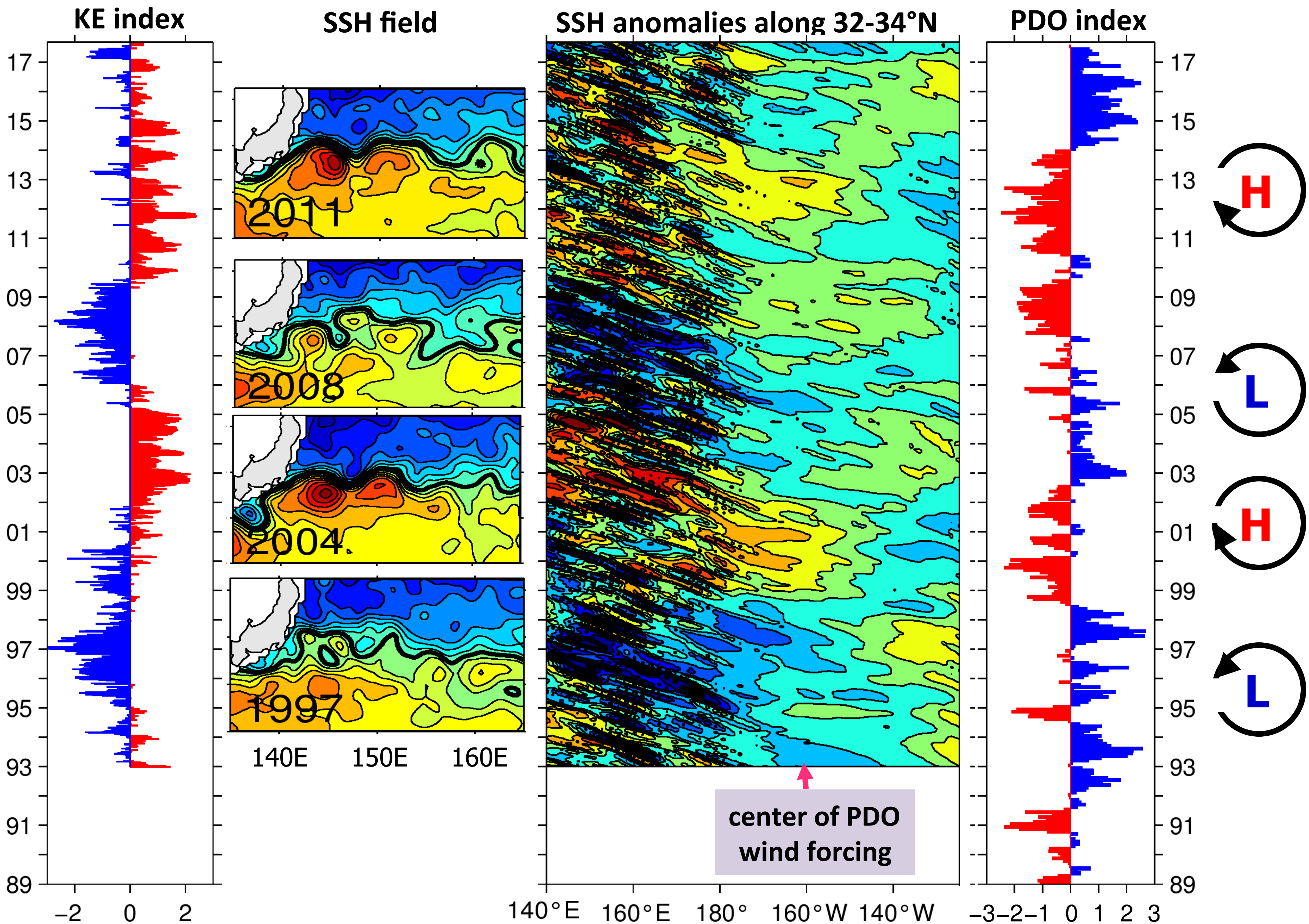

# Quantifying the KE index using a wind-forced linear vorticity model

- Rather than specific climate modes, the proxy KE index is governed by ind . forcing along the 32°-36°N band across the North Pacific basin:

$$\frac{\partial h}{\partial t} - c_R \frac{\partial h}{\partial x} = -\frac{1}{\rho}\nabla \times \left(\frac{\boldsymbol{\tau}_{wind}}{f}\right)$$

- Hindcast of KE index using ECMWF interim Ekman pumping data along the Rossby wave characteristic:

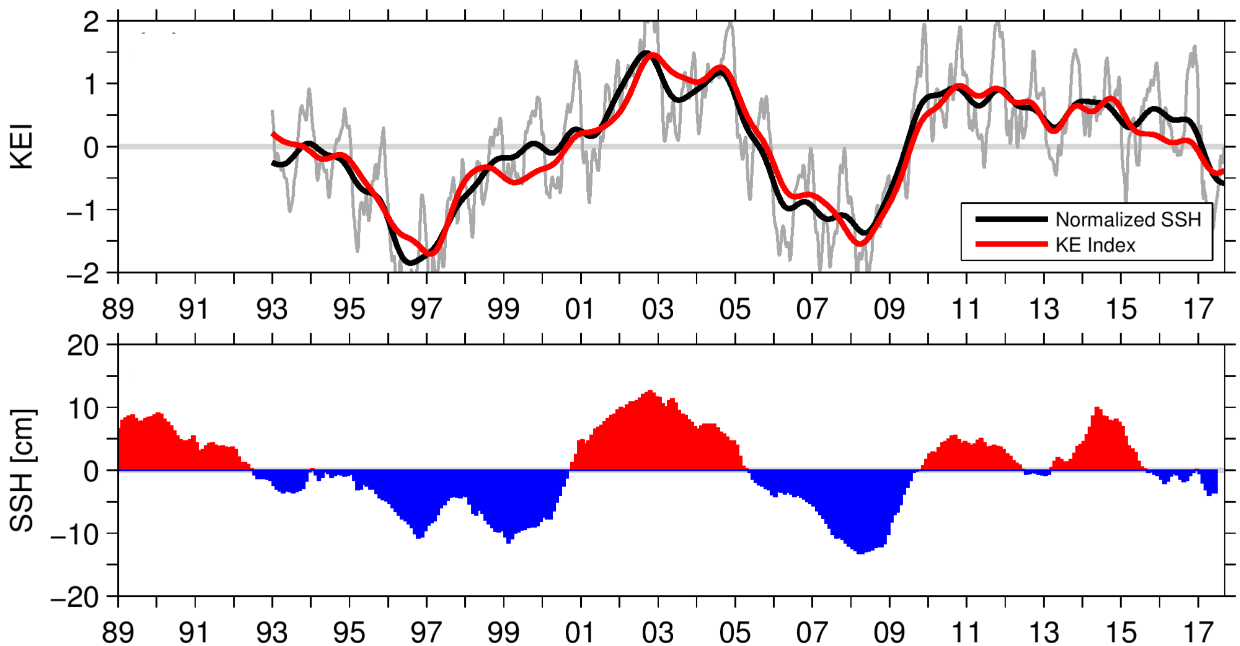


**original time series:**
**r = 0.65**

**low-pass filtered TS:**
**r = 0.87**

# Typical semi-monthly float distributions since the start of the Argo program

**T(z,t)**

**MLD**

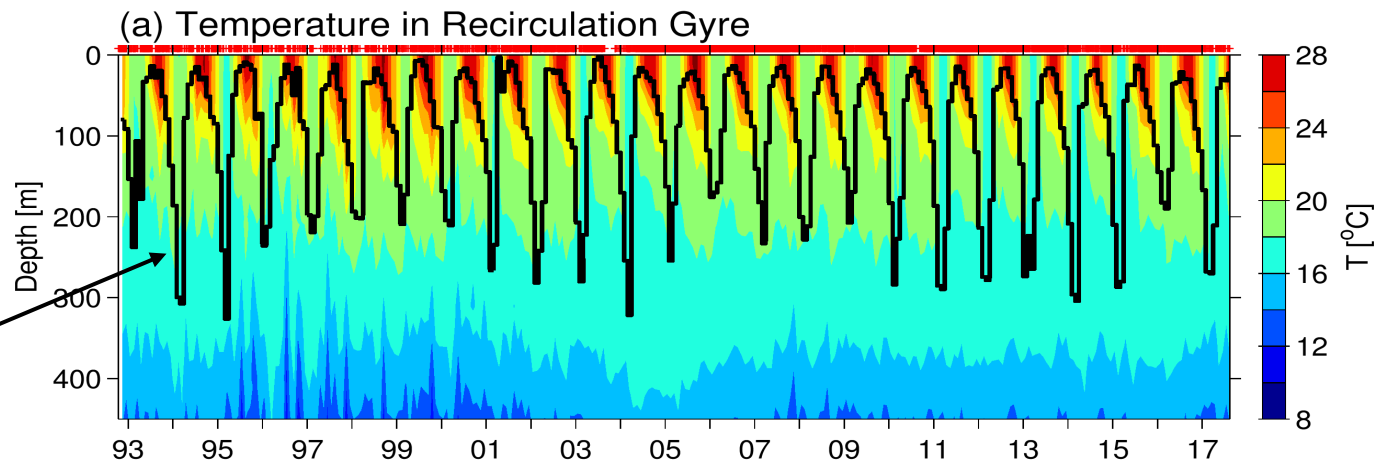


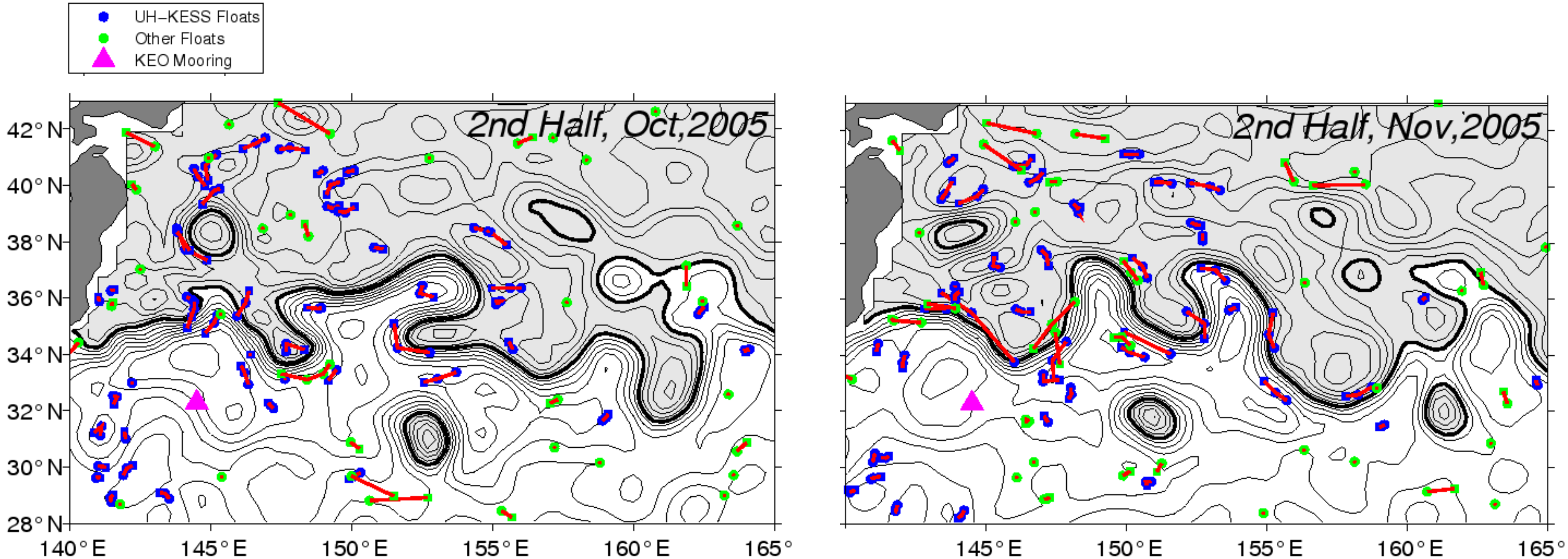

# Float/XCTD/XBT-derived temperature profiles in the KE recirculation gyre

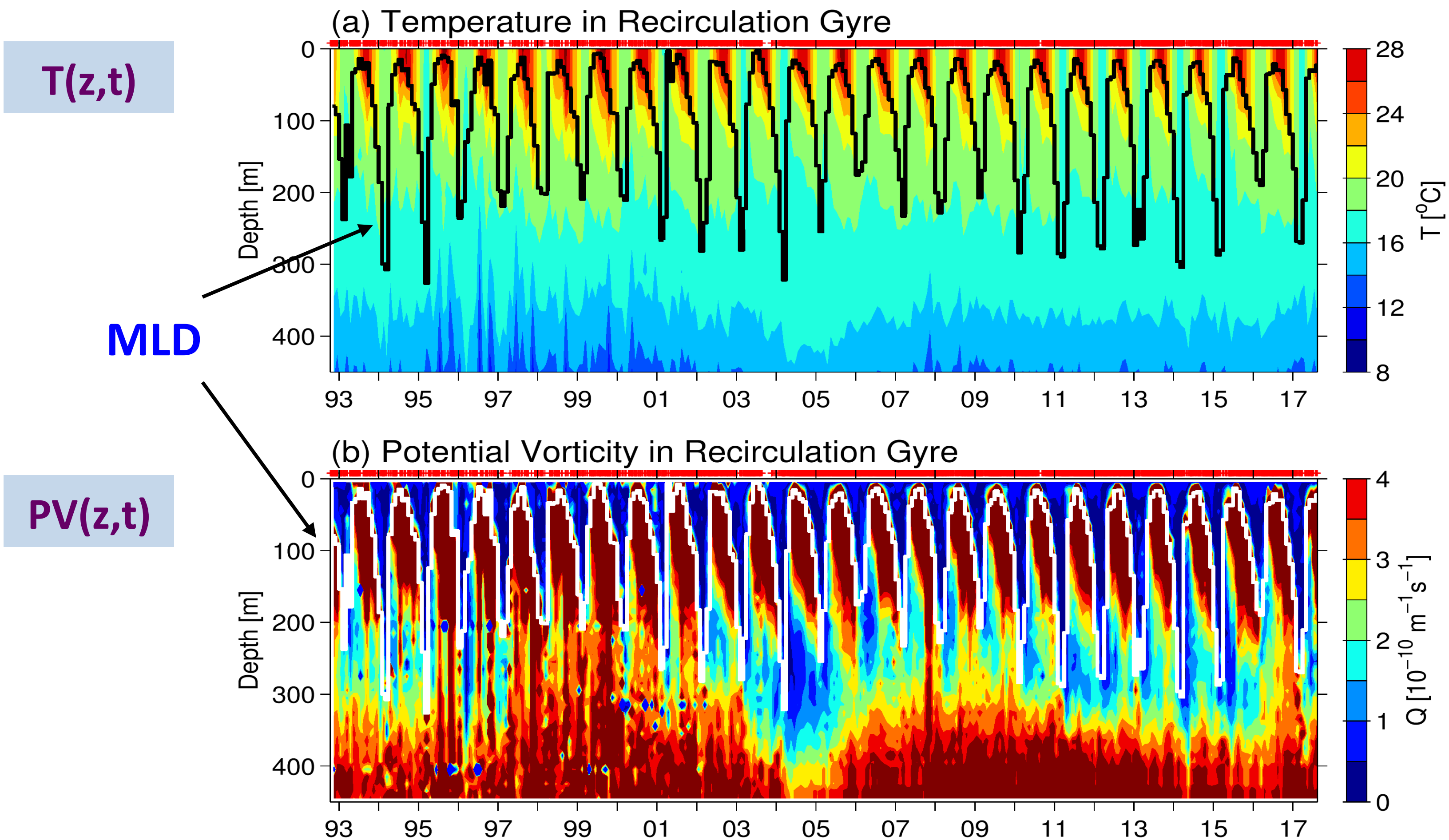


- **STMW is characterized by Q < 2 x $10^{-10}$ $m^{-1}s^{-1}$ below the ML**
- **Deep wintertime ML depth leads to thick STMW formation**
- **ML depth & STMW formation modulate on decadal timescales**

# No clear relationship between wintertime ML depth and heat flux anomalies

**T(z,t)**

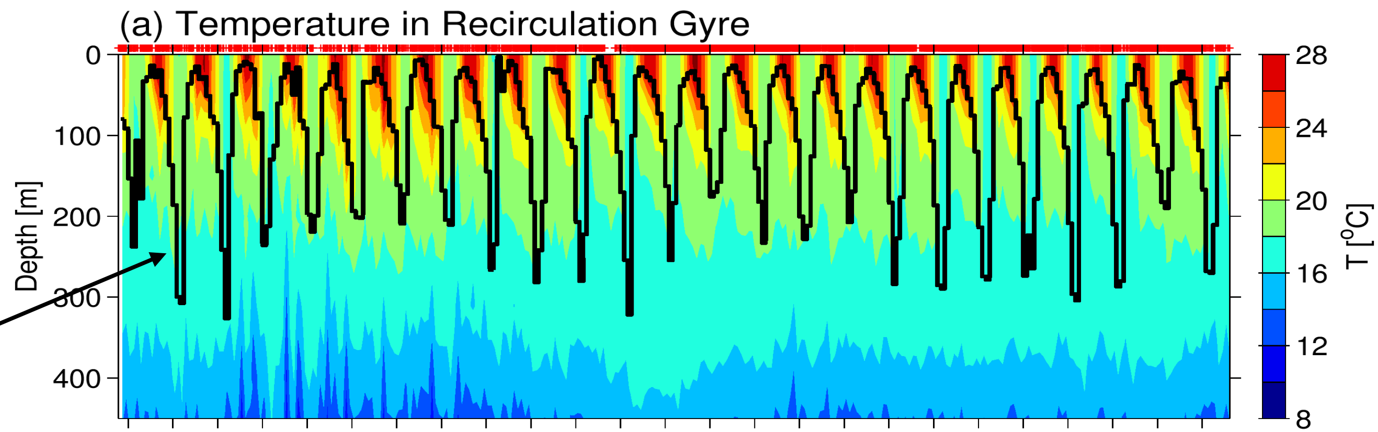


**MLD**

**Q'(t)**

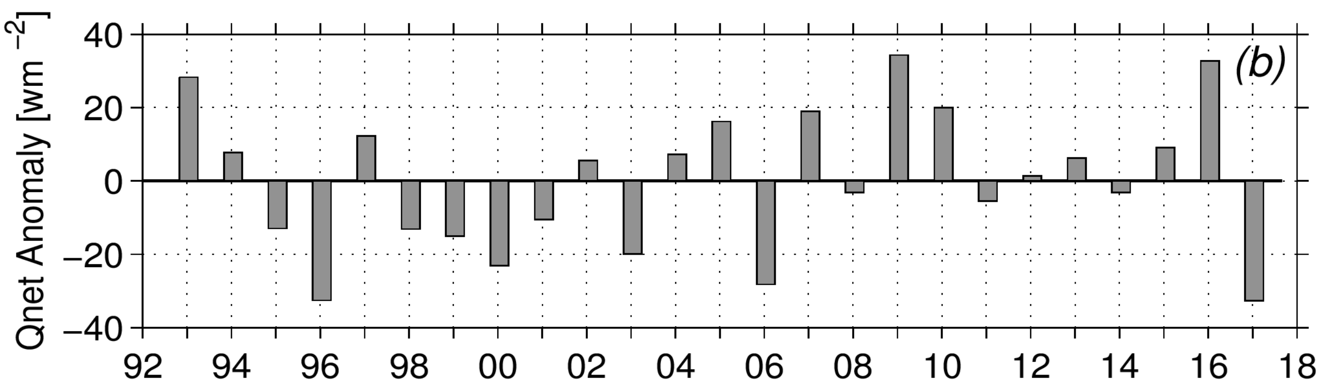


**less cooling**

**more cooling**

**scatter plot for Q' vs. ML depth anomalies**

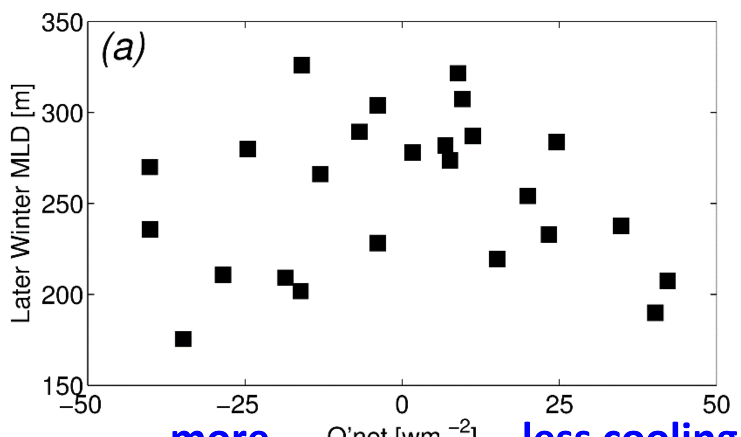


**more**

**less cooling**

# Wintertime ML depth changes are controlled by the KE dynamical state

T(z,t)

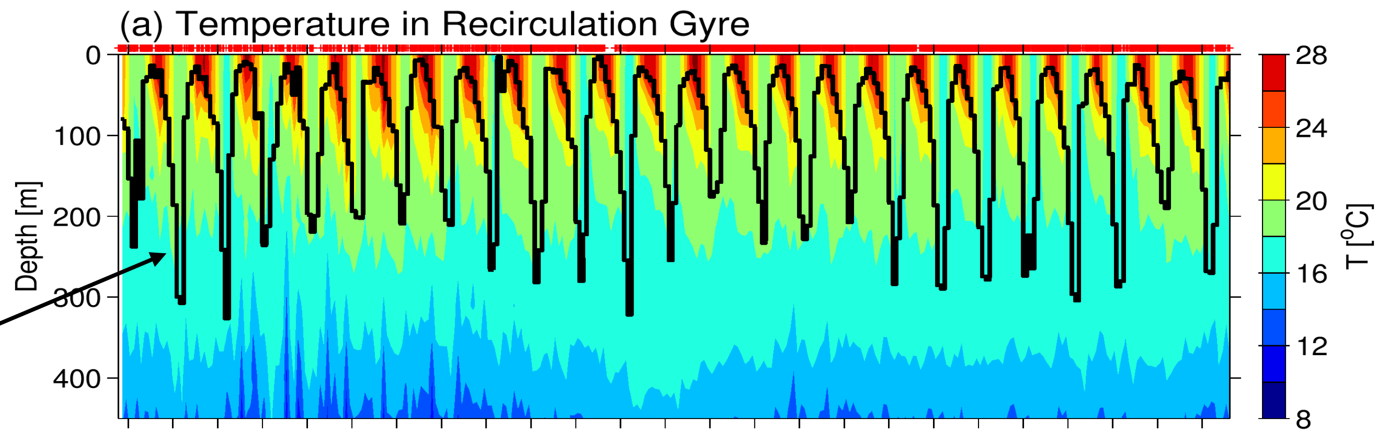


MLD

KE path length

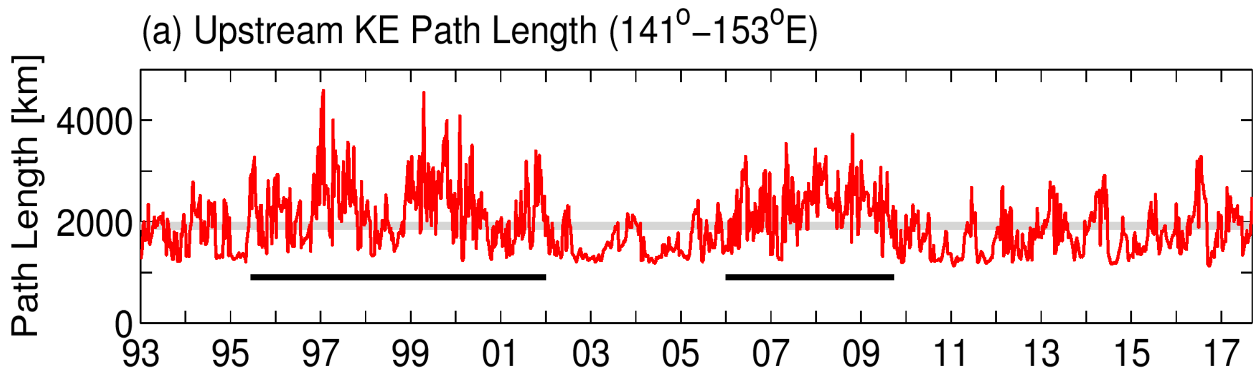


unstable

stable

scatter plot for path length vs. ML depth anomalies

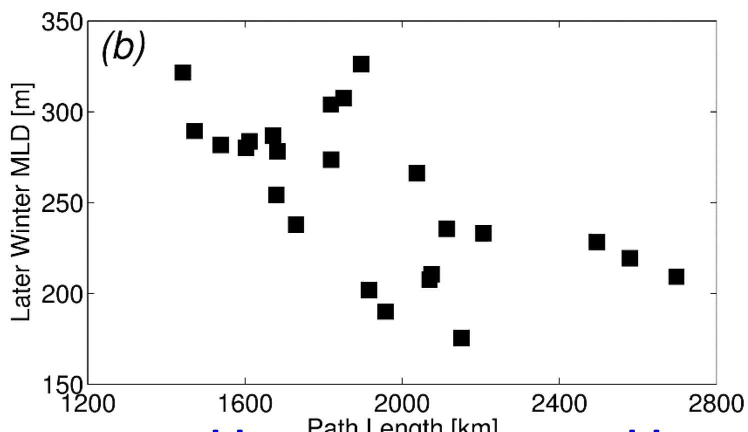


stable unstable

# Factors controlling the late winter mixed layer depth

- Let the fall season upper ocean stratification be ***N*** and let surface cooling be ***Q(t) < 0*** .

- Convective ML depth ***D*** in this case can be estimated from heat conservation in the upper ocean:

$$T(D)\,D - \int_{-D}^{0} T(z)\,dz = \frac{1}{\rho\, c_p} \int_t Q(t)\,dt$$

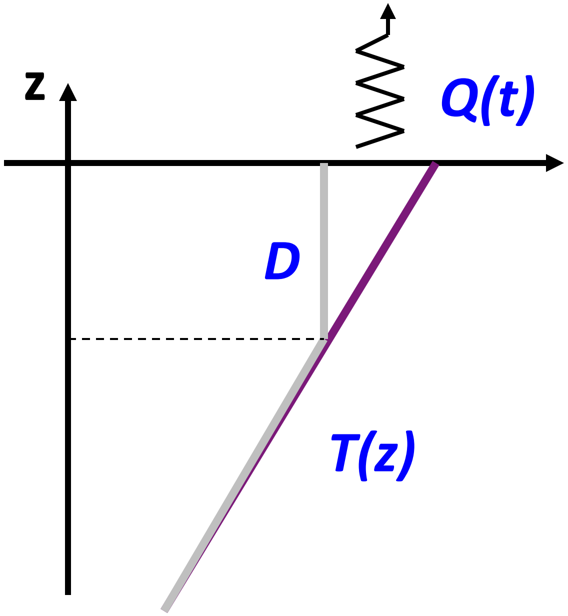


$$D = \frac{1}{N}\sqrt{\frac{-2\alpha\, g}{\rho\, c_p} \int_t Q(t)\,dt}$$

- Convective ML depth depends not only on the cumulative heat loss, but also on the **pre-conditioning stratification, *N***.

Qiu & Chen (2006, JPO)

# KE dynamical state can alter upper ocean stratification efficiently

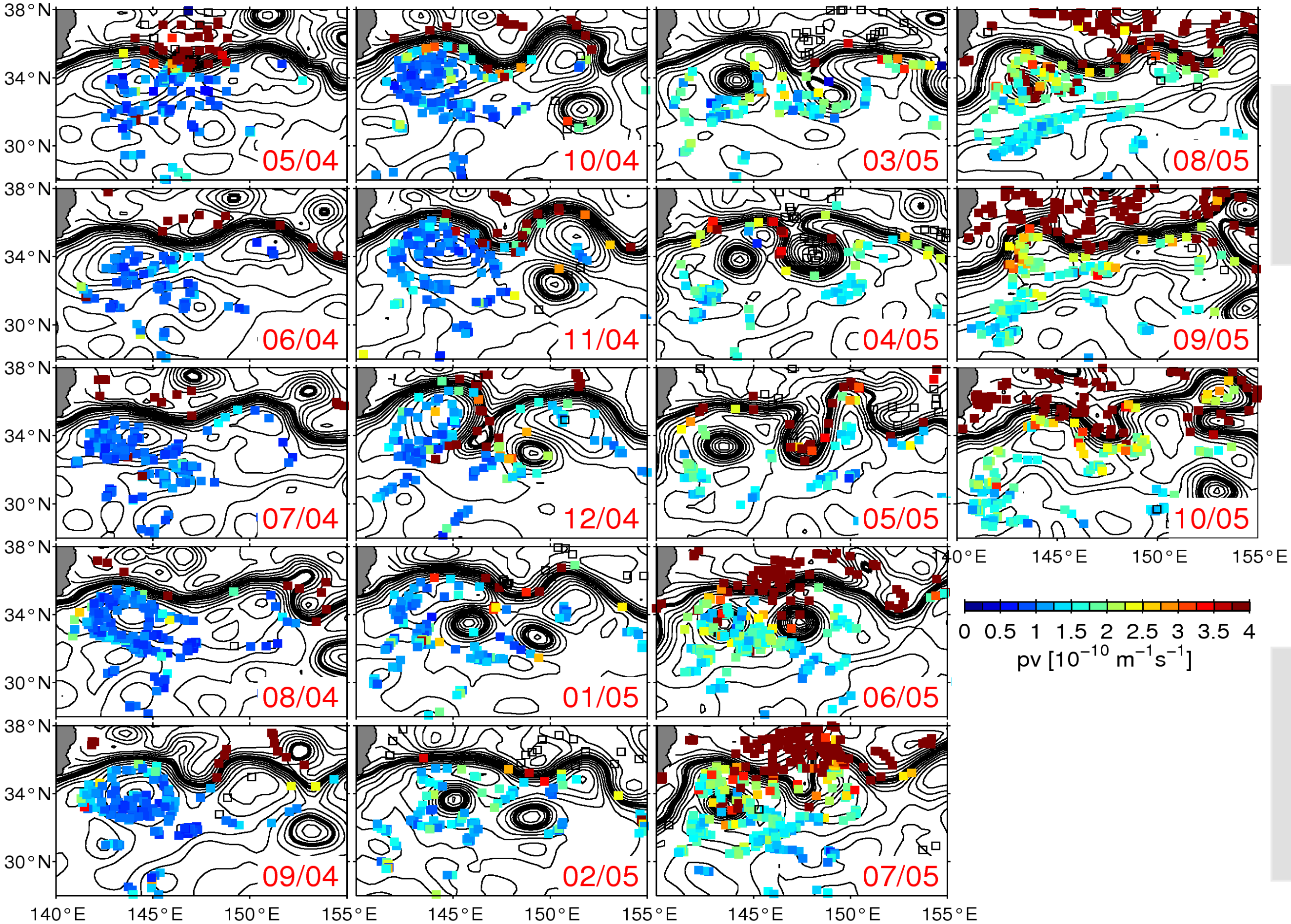


**PV values on 25.4 $\sigma_\theta$ surface (~250m, STMW core) observed by profiling floats**

**Cross-frontal water mass exchanges occur efficiently when KE becomes unstable from 2004 to 2005**

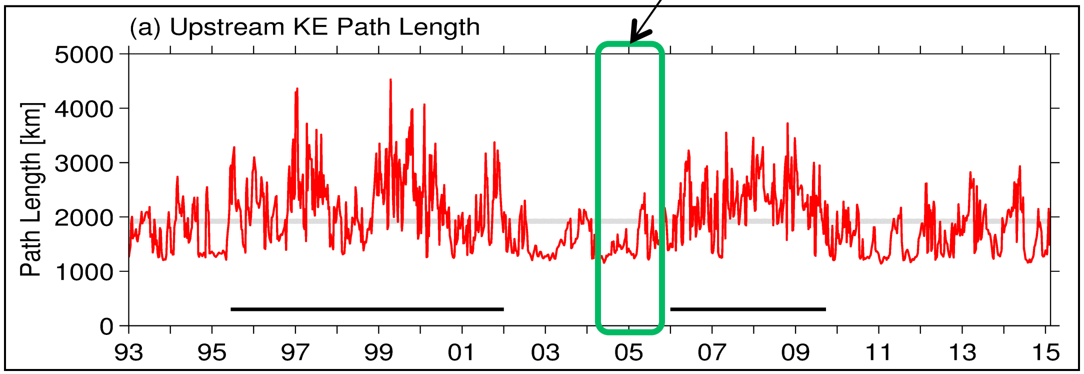


**Qiu et al. (2007, JPO); Bishop & Watts (2014, JPO)**

# Kuroshio/KE supply heat to overlying atmosphere & anchor stormtracks

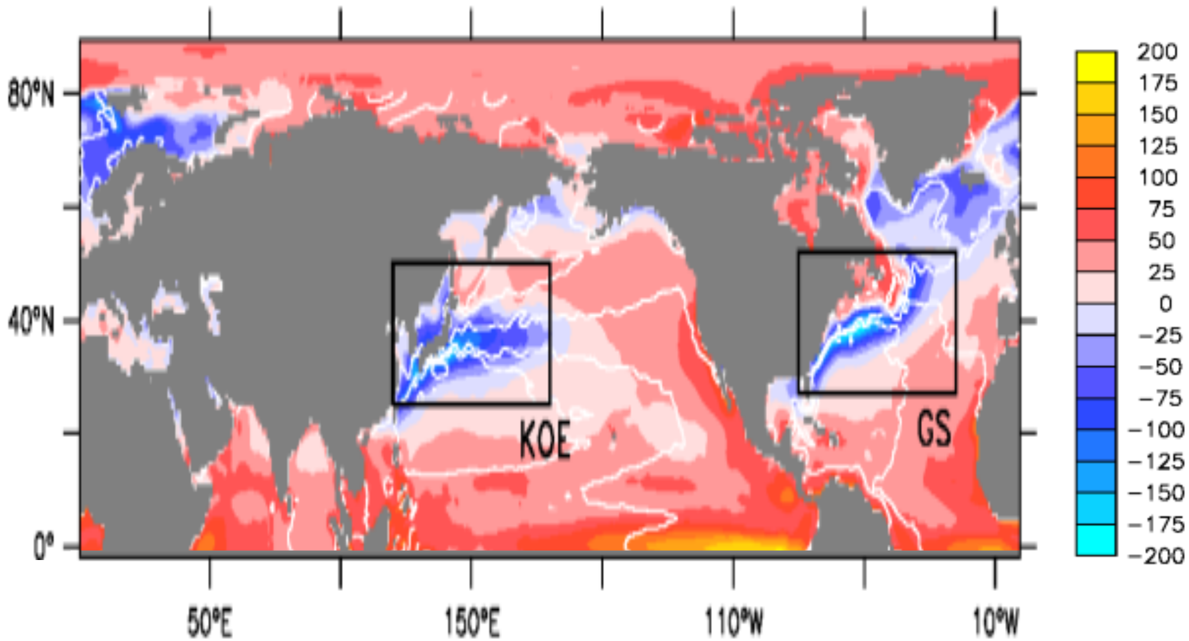


**Time-mean net surface heat flux from air to ocean (W/m$^2$ ; Cronin et al. 2009)**

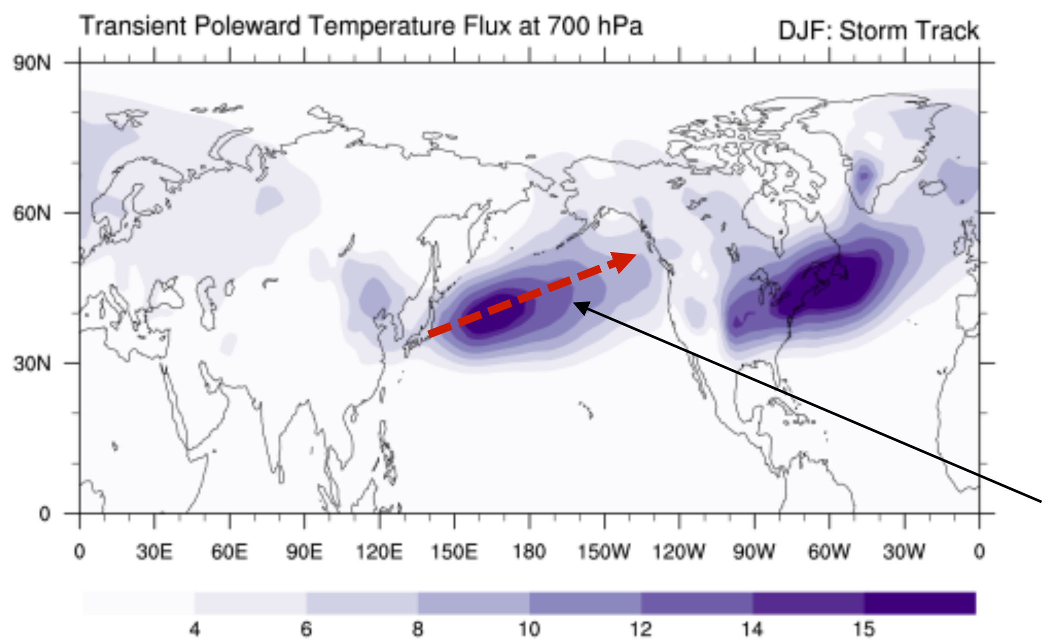


**DJF 700mb rms v'T' fluxes indicative of stormtracks variability (Nakamura et al. 2004)**

**zero wind-stress-curl line/ stormtracks**

# KE dynamic state affects regional SST & cross-front SST gradient

**SST gradient across the KE path**

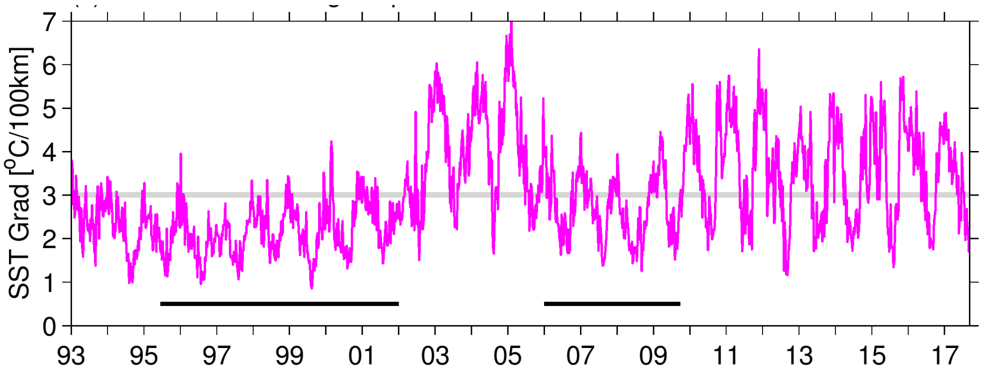


**KE index**

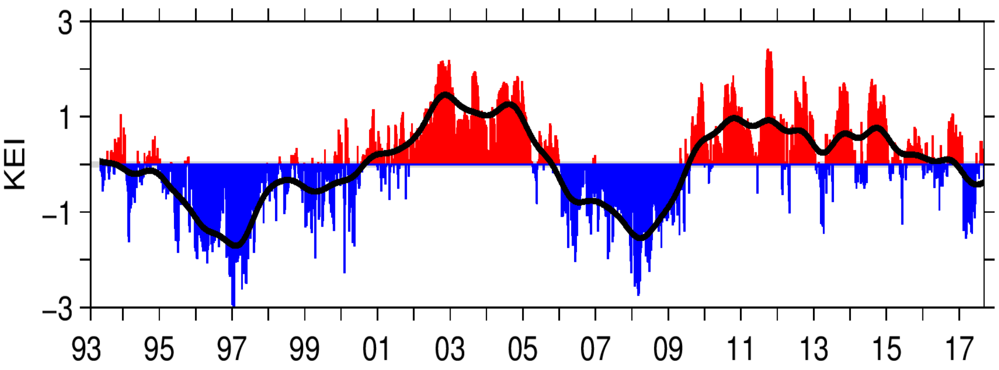


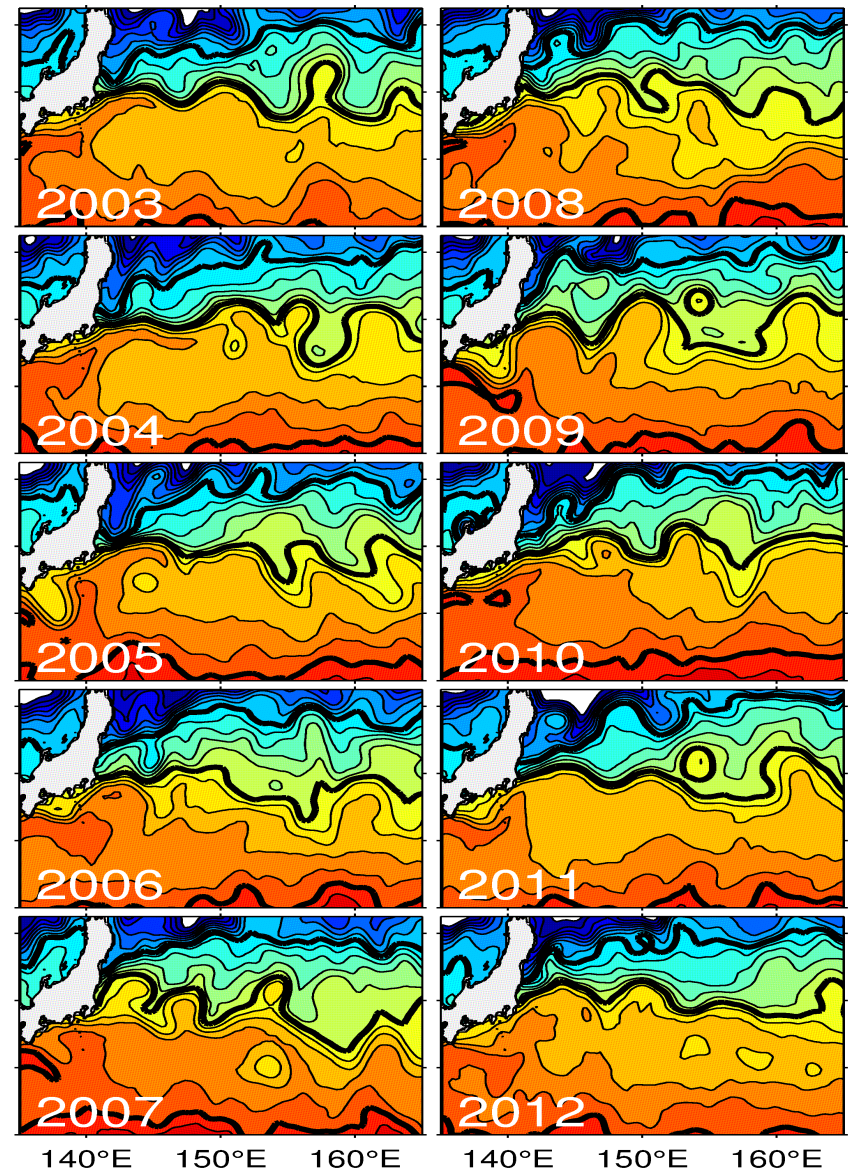


**Feb-March SST maps**

# Basin-scale wind stress curl response to the time-varying KE system

**NCEP mean wind stress curl field**

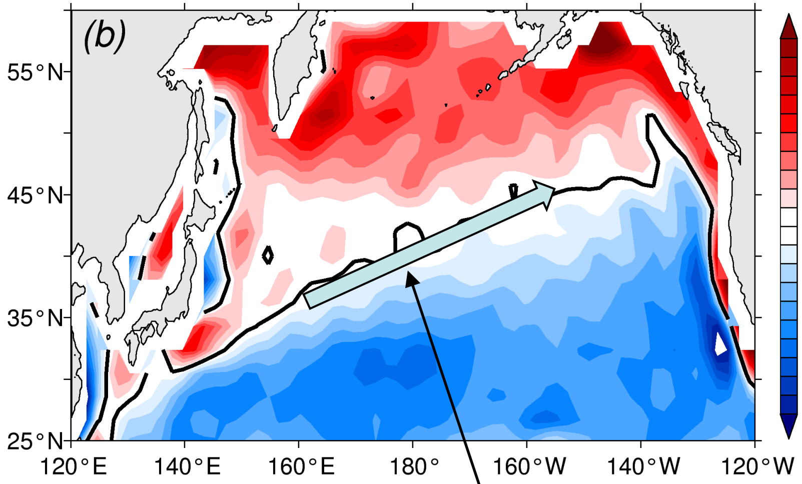


zero wind-stress-curl line/stormtracks

**Anomalous wind stress curls regressed to the KE index of 1977-2012**

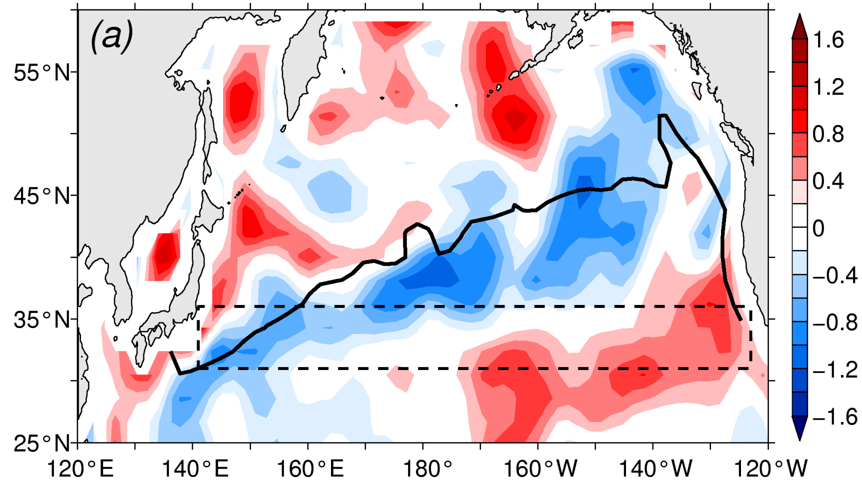


- A positive KE index (i.e., warmer SST & stronger SST front) favors poleward migration of stormtracks/zero wind stress curl line
- This migration causes a dipolar wind stress curl anomaly in 31-36°N band: + in eastern basin

# KE interaction with stormtracks favors a delayed negative feedback loop

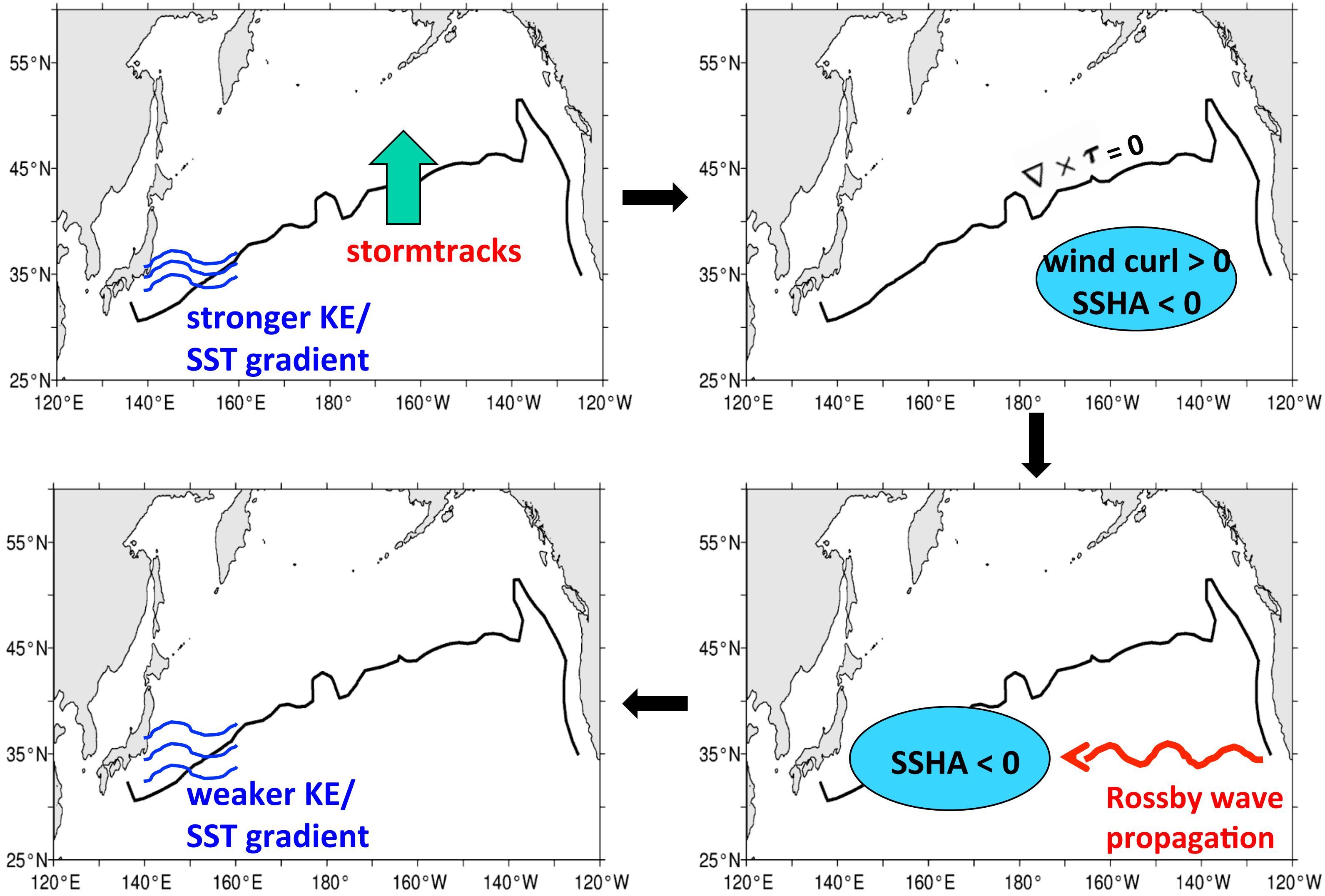


half of an adjustment cycle: ~5 yr across the Pacific basin (Qiu et al. 2014; JC)

# Summary

- KE dynamical state  (i.e. EKE level, path latitude, & KE jet/RG strengths) is dominated by decadal variations.
- SSH anomalies in 31-36°N, 140-165°E provide a good index for decadally-varying KE system; variations of this index are determined by basin-wide wind forcing.
- Decadal KE variability affects STMW properties, SST, & overlying stormtracks.
- A stable KE state induces overlying-high and downstream-low SLP anomalies. This oceanic feedback favors a delayed negative feedback variability with a ~10-yr period.

# Recommendation

- Following the 2013-14 PDO transition, KE is switching from a stable to an unstable dynamical state. **It is timely to conduct a multi-disciplinary Carbon Hot-Spots field campaign to elucidate BGC-physical interactions on air-sea $CO_2$ exchange & carbon export.**

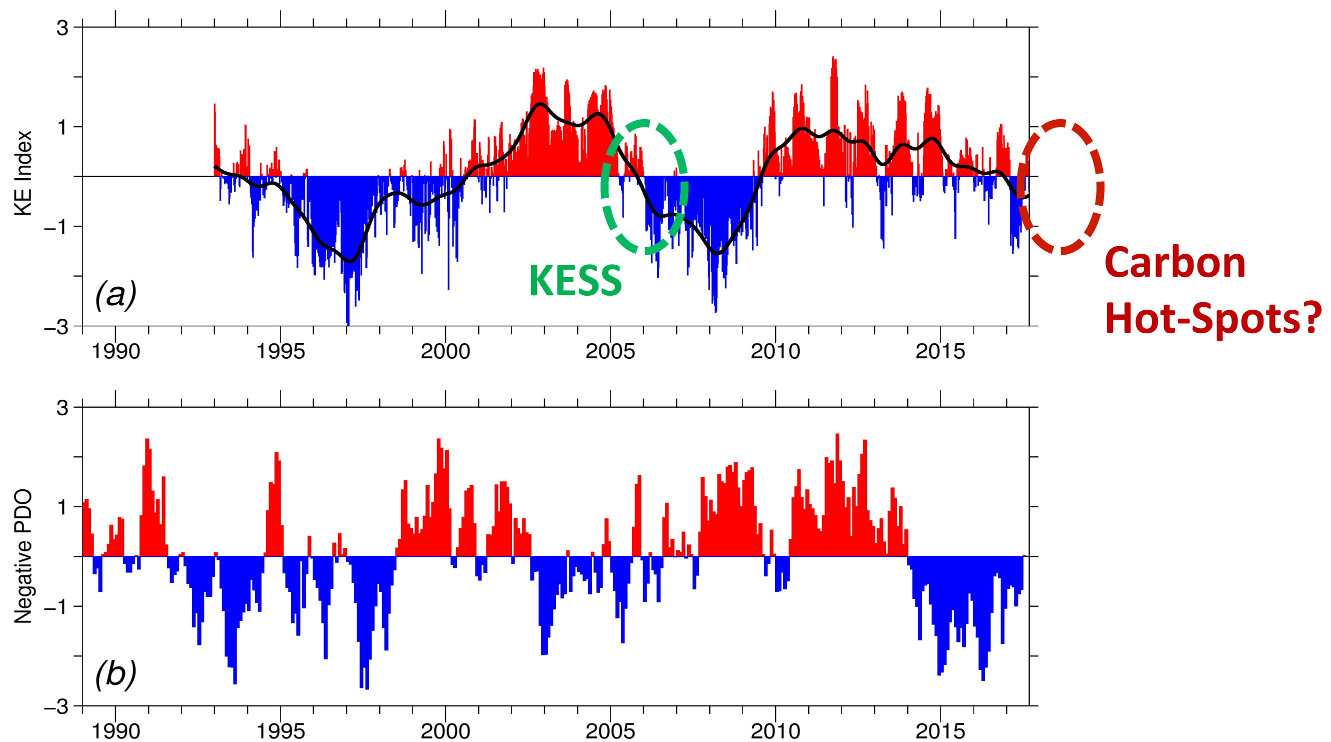

# Basin-scale wind stress curl response to the time-varying KE system

**NCEP mean wind stress curl field**

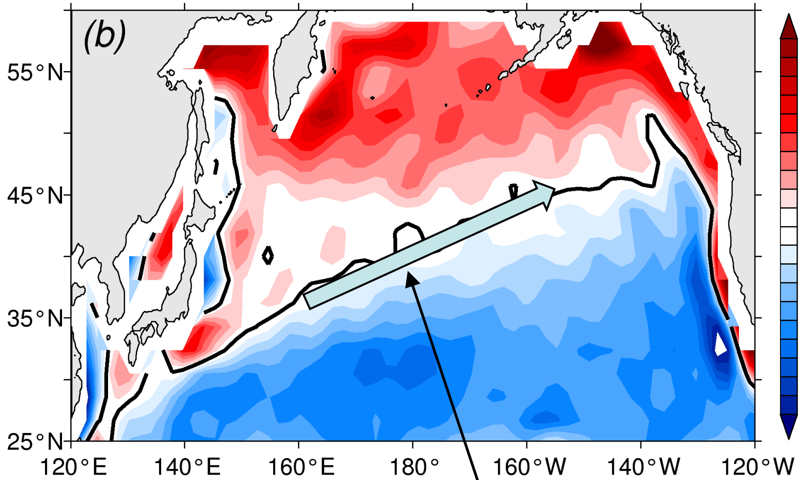


zero wind-stress-curl line/stormtracks

**Anomalous wind stress curls regressed to the KE index of 1977-2012**

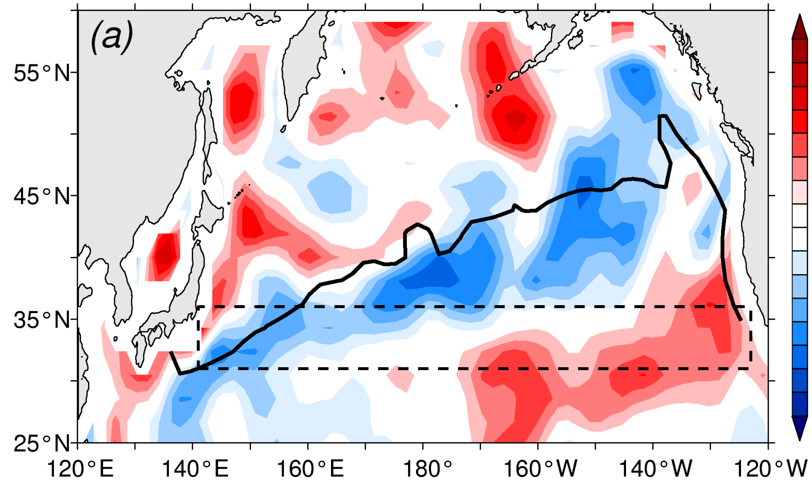


**NDJFM rainfall difference between +/- KEI**

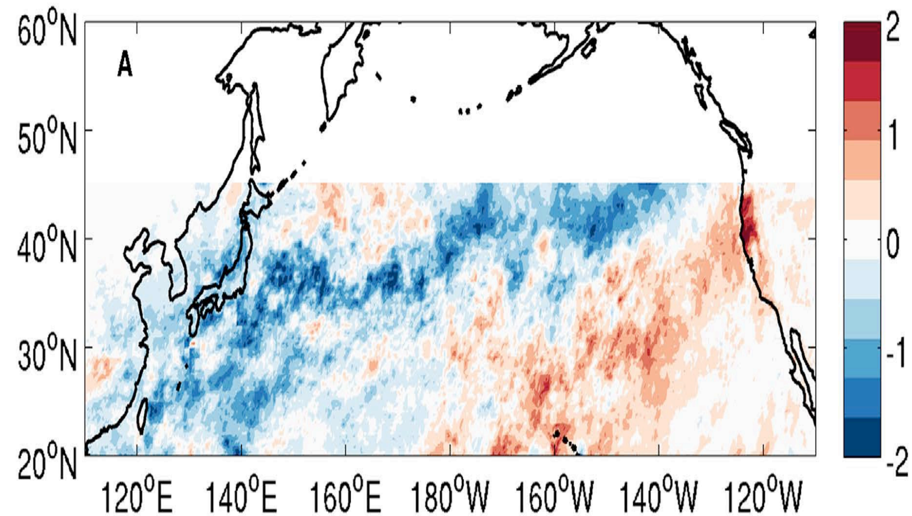


- A positive KE index (i.e., warmer SST & stronger SST front) favors poleward migration of stormtracks/zero wind stress curl line
- This migration causes a dipolar wind stress curl anomaly in 31-36°N band: + in eastern basin
- Consistent evidence from TRMM rainfall data (Ma et al. 2015); potential impact on N America

# Decadal KE variability lags the NPGO index by 2~3 yrs ( r = 0.83 )

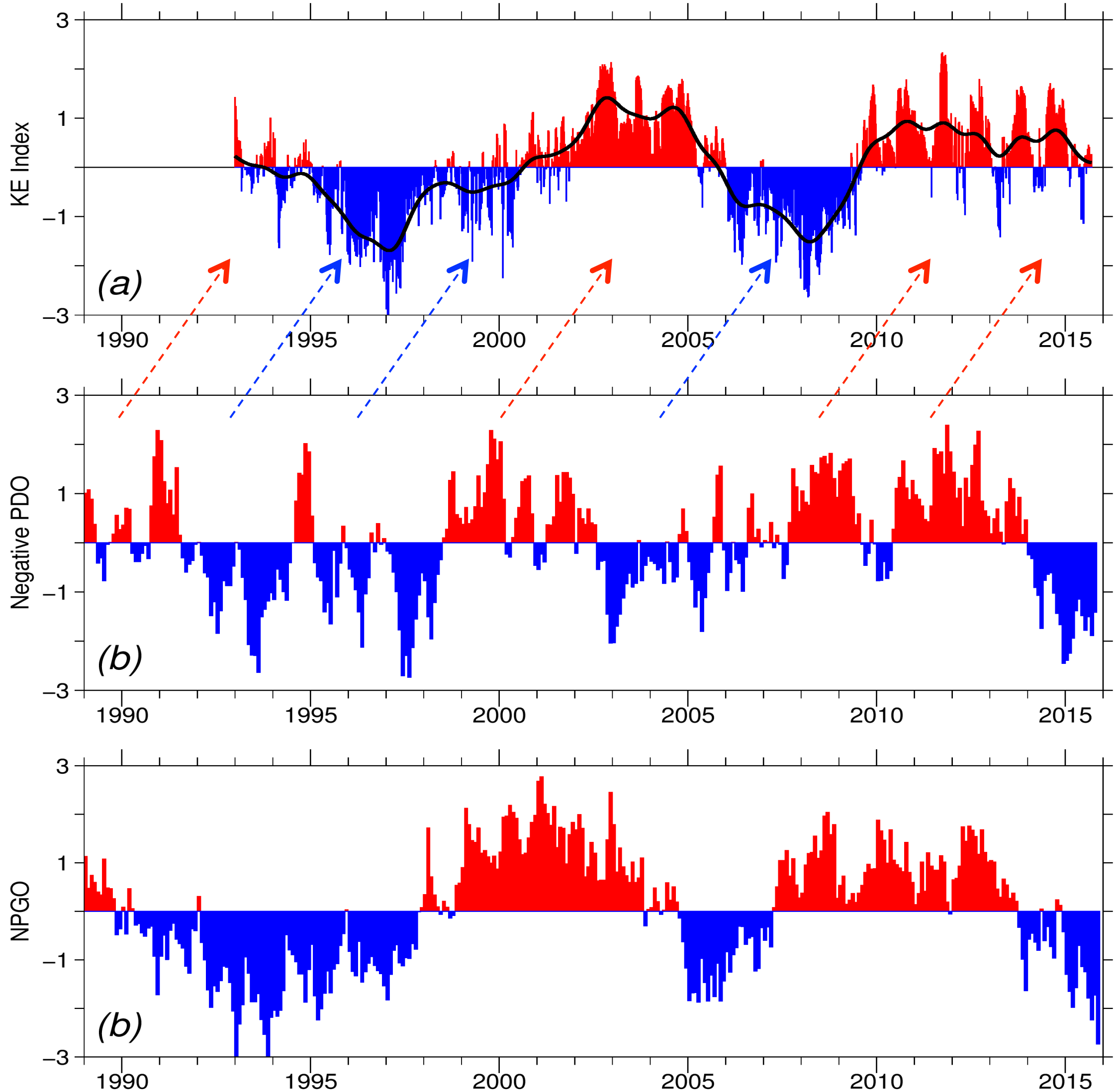


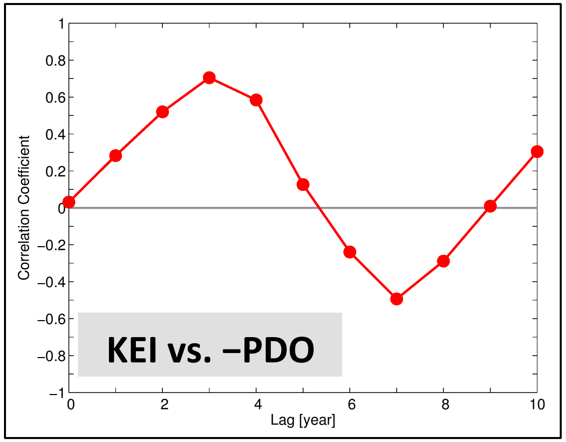


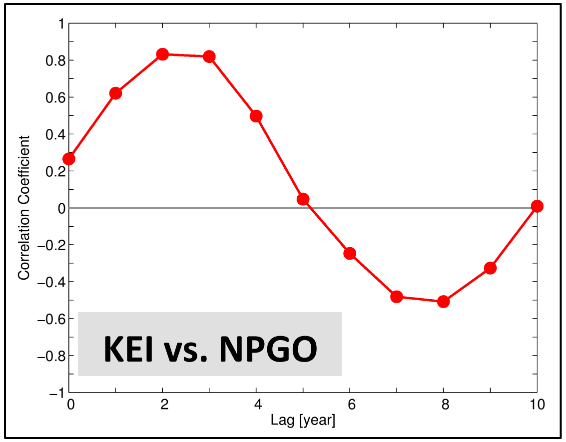


- **NPGO vs −PDO in 1989-2015: r = 0.65**
- **NPGO is SSHA-based and PDO is SSTA-based**

**Di Lorenzo et al. (2008, GRL)**